SOFT ROBOTICS
Volume 00, Number 00, 2025

DOI: 10.1177/21695172251381461

SoRo
Soft Robotics

ORIGINAL ARTICLE

Enabling Tunable Stiffness, Adhesive Grasping, and Interaction-Driven Reconfiguration: A Shape-Memory-Polymer-Enhanced Fin-Ray Gripper

Haotian Guo,[1,*] Hao Wu,[1,*] Yanzhe Wang,[1,*] Yaoting Xue,[2] Tuck-Whye Wong,[2] Tiefeng Li,[2] and Huixu Dong[1]

Abstract

Soft grippers offer a compelling solution for handling tasks in diverse environments due to their inherent safety and adaptability. However, enhancing their versatility, particularly in load capacity and grasping range, while minimizing actuation, remains a persistent challenge. To address this, we propose a soft gripper with reconfigurable morphology, combining structure (Fin Ray Effect [FRE] gripper), and intelligent material (shape memory polymers [SMPs]) as a union, to achieve tunable stiffness, adhesive grasping, and interaction-driven reconfiguration. First, SMPs are integrated into both the front and back beams of the FRE fingers, enabling adhesion grasping and grasping force modulation through phase transition, respectively. Additionally, by leveraging its shape-locking capabilities through intentional environmental interactions, the gripper achieves versatile reconfiguration with a single motor. Besides, inspired by humans interacting with tools and grasping in constrained spaces, we demonstrate three extra grasping modes, including precision pinching, hooking, and corner grasping. Experimental results validate its ability to handle diverse objects, from thin sheets and small nuts to items up to 50 times its own weight. This passive reconfigurable design allows for effective handling of disparate surfaces and contours, guaranteeing safe grasping in constrained spaces. This work opens new possibilities for soft robotic hands, balancing system simplicity with versatility for a wider range of real-world applications.

Keywords: shape memory polymers, soft robotic grippers, tunable stiffness, adhesive grasping, interaction-driven reconfiguration

Introduction

Soft grippers have garnered significant attention for their ability to safely and adaptively grasp objects in real-world applications.[1] However, many current designs are tailored for a limited range of objects or scenarios, and struggle with items that vary greatly in scale, weight, or surface texture.[2,3] Their inherent limitations in stiffness and restricted grasping modes make it difficult to handle larger, heavier objects that exceed the gripper's workspace or designed load capacity. Additionally, achieving stable interactions and grasps in constrained environments imposes further demands on complex actuation and intricate planning, complicating the control of soft manipulators.[4] These challenges highlight the need for enhanced design strategies to improve versatility and performance across diverse grasping tasks while maintaining low system complexity.

Recent advances in stiffness-tunable materials offer a promising pathway to extend the grasping range of traditional soft grippers, especially in enhancing their load-bearing capability. These grippers can accommodate various objects by dynamically modulating rigidity without compromising compliance, achieving enhanced versatility and simplifying control.[2,5] Over the past decades, numerous stiffness-tunable technologies have emerged, including electrorheological (ER)[6] materials, particle jamming,[7,8] low-melting-point alloys (LMPA),[9] shape memory alloys (SMAs)[10] and polymers (SMPs),[2,11–14] etc. Among these, jamming-based approaches leverage frictional locking to

[1]Grasp Lab, Department of Mechanical Engineering, Zhejiang University, Hangzhou, China.
[2]Center for X-Mechanics, Department of Engineering Mechanics, Zhejiang University, Hangzhou, China.
*Haotian Guo, Hao Wu, and Yanzhe Wang contribute equally to this work.

transition granular materials from deformable to rigid, enabling simple yet versatile grasping.[7,8] However, their insufficient grasping force and precision hinder their suitability for fine tasks. ER-based systems demonstrate rapid response times, with the ER effect manifesting in milliseconds.[15,16] Whereas sustaining high stiffness demands constant high voltage, resulting in significant energy consumption.[17] Moreover, their limited maximum stiffness restricts their effectiveness in high-load applications.[16] SMAs, though offering good structural rigidity, present only a narrow (≈2.3×) stiffness variation.[18] In contrast, thermally activated SMPs offer a more promising alternative, with tunable stiffness ranging from a few MPa to several GPa.[2,14] For instance, inspired by the bones and joints in human fingers, Yang introduced SMP-based joints that achieved a 24.9× joint stiffness modulation, improving the precision of position control in soft robotic hands.[3] By incorporating a high concentration of Schiff-base bonds into the epoxy crosslinking network, Peng achieved exceptional shape memory and self-healing capabilities, with a mechanical strength 50 times their own weight.[14] Moreover, SMPs retain high stiffness at ambient temperatures, significantly reducing energy consumption.[12,14,19] Furthermore, SMPs unexpectedly exhibit adhesion capabilities through microscopic interlocking effects during phase transitions,[13,20] enabling soft grippers to handle flat and tiny objects with ease, making them particularly well-suited for this study.

Another challenge in enhancing soft robotic hands' versatility and grasping capabilities involves the structural design. Various structural and actuation principles have been explored.[1,21,22] For instance, Cui employed pneumatic actuators that independently control distance, angle, and finger flexion of a soft gripper, expanding its grasping range through dynamic initial posture adjustment.[1] Based on the antagonistic configuration of extensor and contractor McKibben muscles, Loai constructed a soft robotic arm, enabling increasing structural stiffness without affecting finger positioning.[21] Some studies focus on anthropomorphic designs to achieve human-like dexterity. For instance, Konda et al. employed 11 actuators to drive a 6-Degree-of-Freedom(DOF) soft hand, replicating 31 out of 33 grasps from the Feix GRASP taxonomy.[22] Despite their advancements, such systems often require bulky and complex actuators, complicating both control and maintenance. Achieving versatile grasping with minimal actuation remains a critical issue.[13] In contrast, underactuated grippers, such as Fin Ray Effect (FRE) grippers,[23] or underactuated linkage grippers,[24] aim to extend the grasping range via simplified designs. In particular, FRE grippers have been widely used in industrial settings for their adaptability to diverse objects.[25,26] However, most underactuated grippers exhibit limited grasping modes and are often tailored for specific loading ranges, limiting their ability to handle the diversity encountered in daily scenarios.[23,27] As such, there is a growing need for soft grippers capable of handling a broader range of forces and offering more grasping modes to meet this demand.

Motivated by these unresolved issues, this study presents a novel gripper actuated with one motor. This design achieves versatile grasping with minimal actuation by fully leveraging the adhesion and tunable stiffness properties of SMPs. First, SMPs are strategically placed on two contact surfaces of FRE structure. The front SMP layer permits extra adhesion-based grasping while the dorsal SMPs enable stiffness modulation to handle wider forces, reduce motor load, and improve precision. Inspired by human grasping in various scenarios, the gripper can dynamically reconfigure its morphology through intelligent interactions with the environment, further expanding its grasping modes. We highlight the key novelties of our work. Foremost, the core contribution lies in developing a novel soft gripper actuated by a single motor, which remarkably enables diverse grasping across a wide range of objects and constrained environments, offering significant potential for applications concurrently requiring compliance and precision. In particular, the contributions of this work are threefold. First, we introduce a novel SMP-enhanced soft FRE gripper with stiffness modulation and adhesion-based grasping capabilities. This integration leverages the unique properties of SMPs to extend the gripper's adaptability and grasping versatility. Second, the gripper achieves flexible reconfiguration through deliberate interactions with the environment, where new morphology is maintained through SMPs' rubber-to-glass (R2G) transition. The shape fixation ratio is quantitatively evaluated, demonstrating the gripper's ability to reconfigure. Third, a human-inspired segmented stiffness modulation strategy is proposed, enabling diverse grasping modes, including precision pinching, hooking, and corner grasping. Experimental results validate the gripper's outstanding performance and versatility across varied physical environments. These innovations highlight the versatility and efficiency of the SMP-enhanced FRE gripper, providing an adaptable solution for robotic applications that require multifunctional grasping capabilities.

Characterization of the SMP Material

Thermal-responsive SMPs exhibit a highly tunable elastic modulus, temporary shape-locking and permanent shape-memory effect when transitioning between different phases.[19] The stiffness ranges from surpassing 1 GPa in the glassy state to around 1 MPa in the rubbery state, dropping by three orders of magnitude. Additionally, deformation in the rubbery state can be retained through R2G transition, termed shape-locking. Upon reheating to temperatures surpassing the glass transition temperature T_g, the polymer reverts to its primary configuration, demonstrating the shape-memory effect. The variance in stiffness enables SMPs to provide reliable locking and easy embedding of objects, making them ideal for applications requiring variable stiffness and surface adhesion. Prior research has predominantly focused on a single aspect of SMPs, either adhesion or variable stiffness characteristics. The work aims to fully leverage these properties by integrating them with a passive shape-adaptive gripper to enhance its versatility in grasping and manipulation.

Material and sample preparation

A thermal-triggered epoxy SMP[13] is employed. The fabrication process involves mixing the epoxy monomer (E44 6101) with the curing agent (JEFFAMINE D-230, Aladdin) in a mass ratio of 81:46. The mixture is cast into pre-designed silicone molds. After curing in an oven initially at 50°C for 2 h, followed by 100°C for 2 h, and post-curing at

130°C for another 2 h, the SMP substrate is obtained upon demolding.

Stiffness-tunable behavior of the SMP

To investigate the thermomechanical behavior of the E44 SMP, we conducted dynamic mechanical analysis (DMA) with a Q800 analyzer. The temperature was raised from 20°C to 120°C at 3°C/min. Figure 1A illustrates the DMA results. The T_g of the SMP was identified at approximately 48.6°C, based on the peak of tanδ, which represents the loss modulus to storage modulus ratio. This relatively low transition temperature enables object manipulation with minimum risk of thermal damage. The storage modulus, reflecting the elastic response, decreased significantly from 1.26 GPa at room temperature to below 10 MPa at temperatures above 80°C, indicating a transition from the glassy to the rubbery state. Besides, the wide stiffness variation range of E44 SMP enables the integration of shape adaptability with load-bearing capacity. Figure 1B shows SMP's load-bearing performance under varying conditions. At room temperature, the SMP strip (20 × 100 × 3.5 mm) exhibits high stiffness,

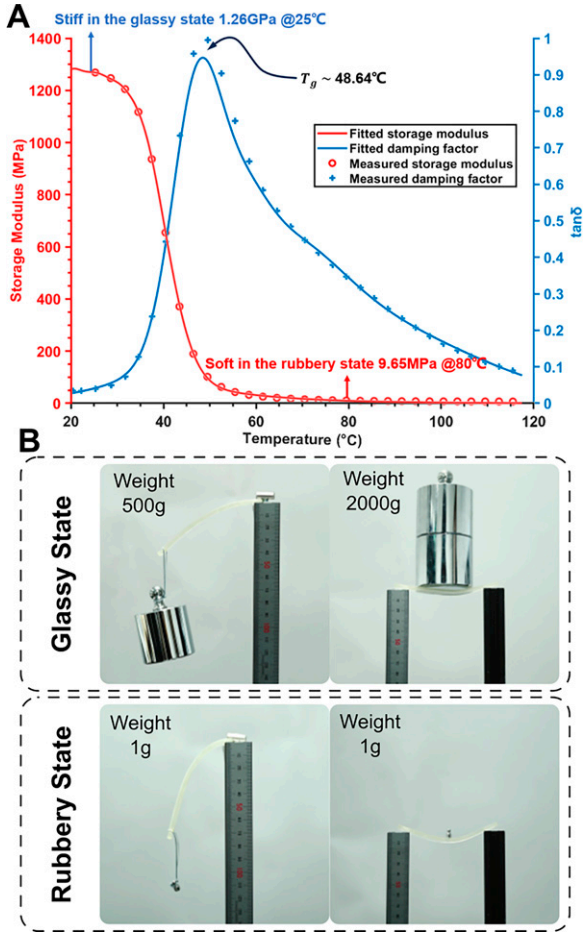

FIG. 1. Stiffness-tunable behavior of the SMP material. **(A)** The DMA characterization of the E44 epoxy SMP (Test frequency 1 Hz, temperature rising rate 3°C/min). **(B)** Demonstration of the stiffness variation of the thermally activated SMP material at 25 and 80°C. DMA, dynamic mechanical analysis; SMP, shape memory polymer.

effectively resisting bending under a load of 500 g in the cantilever beam configuration and 2 kg in the simply supported beam configuration. In contrast, the bending deflection significantly increases in the rubbery state, indicating a greatly reduced stiffness and good adaptability, where the SMP merely supports 1 g in both configurations.

Adhesion evaluation of the SMP

The E44 SMP demonstrates adhesiveness via thermally responsive phase transitions. The behavior occurs following the R2G transition upon contact with the substrate, creating a robust mechanical interlock with the surface. The SMP reverts to its initial configuration when reheated, effectively disengaging the previously secured adhesion. The R2G mechanism allows for controlled, reversible adhesion in response to thermal stimulus. To quantify this adhesion strength, we developed a cable-based adhesion measurement platform, as depicted in Figure 2A. Here, we distinguished between the influence of target surface texture and contour on adhesion strength. SMP samples (20 × 30 × 3 mm) were prepared following stated procedures. During each test, the sample was first heated above 80°C with a heating stage to transition it into a rubbery state, establishing conformal adhesive contact with the target surface under a preload of 1 kg. It was then cooled to room temperature under the same preload until transitioning to the glassy state. An upward pull was applied using water-filled weights until detachment, with the maximum force per unit area used to calculate adhesion strength.

Figure 2B shows the adhesion measurements of the SMP on substrates with different materials. Despite variations in surface roughness, the SMP exhibited robust adhesion across all materials, with forces far exceeding the applied preload. To isolate the effect of surface curvature on adhesion, SMP samples with convex, flat, and concave surfaces were further tested on objects with varying geometries, all fabricated from the resin material to control for material-related influence. Figure 2C demonstrates that the ability to adjust SMP morphology enhances grasping performance on objects with varying surface geometries. Notably, contact area plays a critical role in adhesion strength. Compared with sawtooth and wave profiles, flat plates exhibited a 240% increase in adhesion. The highest adhesion was measured when concave SMPs gripped convex targets, due to the maximized contact area. Meanwhile, this microscopic interlocking occurs not only at the contact interface but also along the lateral surfaces, which explains why SMPs achieved adhesion forces twice the preload even on surfaces with minimal contact areas, such as sawtooth and wave profiles. These experimental results underscore that optimal adhesion strongly depends on shape conformability.

Construction of SMP-FRE Gripper

Design of SMP-FRE gripper

Integrating SMPs with FRE fingers offers a novel approach to soft gripper design. Previous study explores modulating the grasping force of Festo FRE grippers by altering the stiffness of the front beam using a jamming-based mechanism.[28] While SMPs outperform it by providing thermo-responsive stiffness modulation and extra reversible adhesion, they require

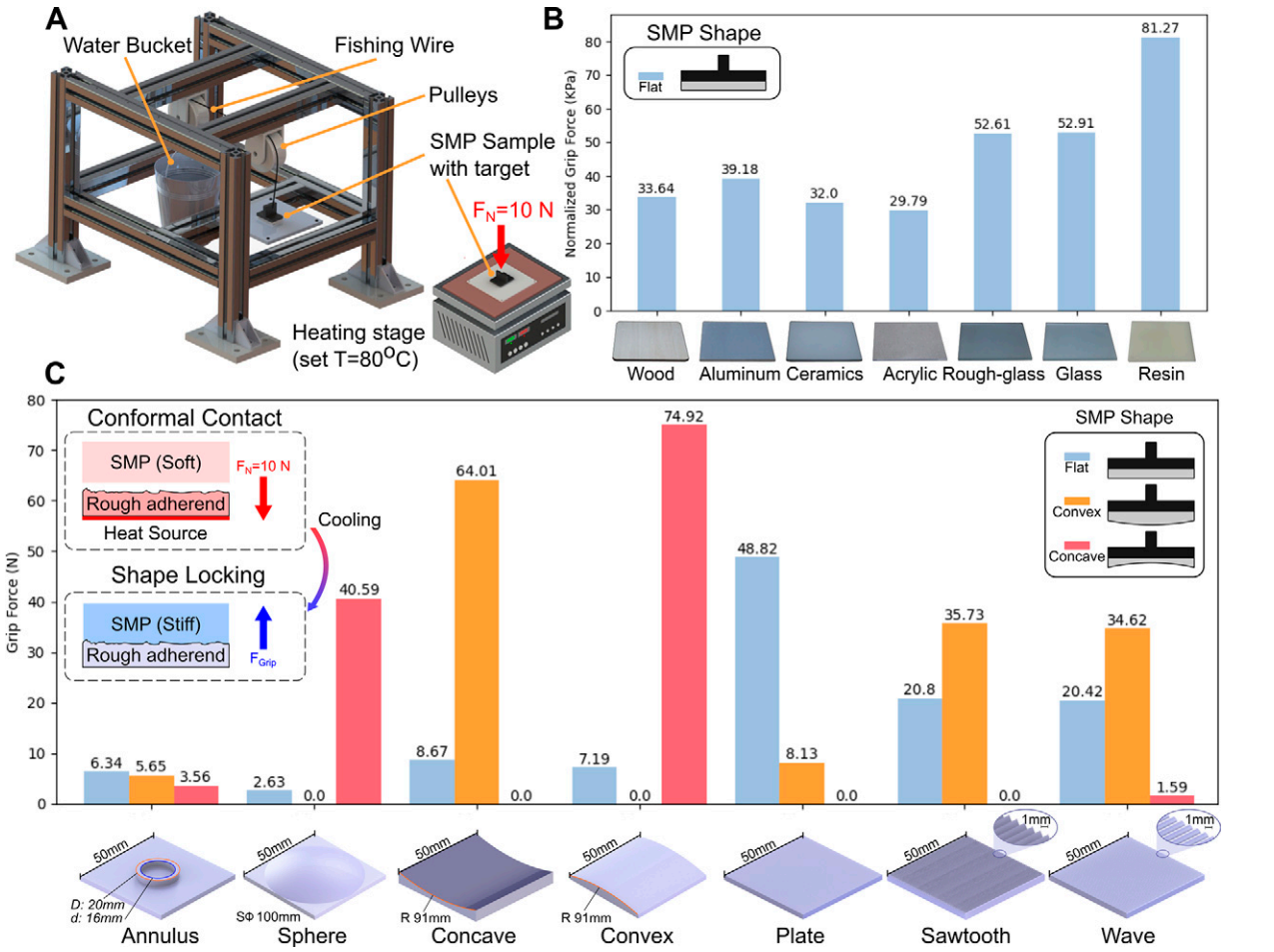

FIG. 2. Adhesion performance of the SMP material to objects with various materials and arbitrary shapes. **(A)** Setup for measuring the normal adhesion strength of the SMP sample. **(B)** Grip force to planar objects of different materials: wood, aluminum, ceramics, acrylic, rough glass and smooth glass (length 100 mm, width 100 mm, thickness 3 mm). **(C)** Grip force of SMP with flat, concave and convex surfaces to objects with different shapes: annulus (diameter, 20 mm), sphere (diameter, 100 mm), concave (diameter, 182.5 mm), convex (diameter, 182.5 mm), sawtooth (triangular serrations with a side length of 1 mm), wave (semicircular waves with a diameter of 1 mm).

temperatures well above the glass transition temperature (T_g) to function efficiently in practical applications. This presents a risk of potential heat damage during interactions if SMPs are positioned at the front. As prior study reveals, the virtual work of FRE structure's deformation consists of the deflection of the front beam, the deformation of the front and back beams at their joints, the compression of the crossbeams by passive torques, and the actuation force on the clamped crossbeam that moves the entire finger.[29] In such closed-chain structures, stiffening either the front or back beam reduces deformation, indicating higher structural stiffness and enabling higher grasping forces. Therefore, the variable stiffness SMP is strategically placed on the back contact side of the FRE structure, with the front SMP kept thin to preserve flexibility and conformability. This arrangement entitles the finger to adhere to the object while adjusting its segmented structural stiffness. Additionally, the SMP-FRE gripper can reconfigure and maintain its shape through intended interactions with the objects or environment, providing a versatile grasping and manipulating solution for a wider range of objects with varied sizes, weights, and shapes.

Figure 3A presents an overview of the proposed SMP-FRE gripper, comprising two identical FRE fingers. A single stepper motor actuates the gripper through a linkage-based transmission, enabling a 180° range of motion from fully open to fully closed. Each finger contains dual SMP material layers, corresponding electroheat layers, and K-type thermocouples. The segmented electroheat pieces, each rated at 5W, enable independent heating of the SMP sections, modulated by a voltage regulator via PWM. Meanwhile, 8-channel K-type thermocouples, operating at 30 Hz, monitor the temperature of each SMP segment to ensure precise local stiffness regulation and operational safety. Figure 3C and D details the gripper's geometric dimensions and electronic control system. A PID controller modulates individual heating elements through PWM to maintain the desired temperatures.

Fabrication

Traditionally, fabricating SMP separately and subsequently attaching it to thermoplastic urethane (TPU) introduces interfacial mechanical weaknesses, as the adhesive layer

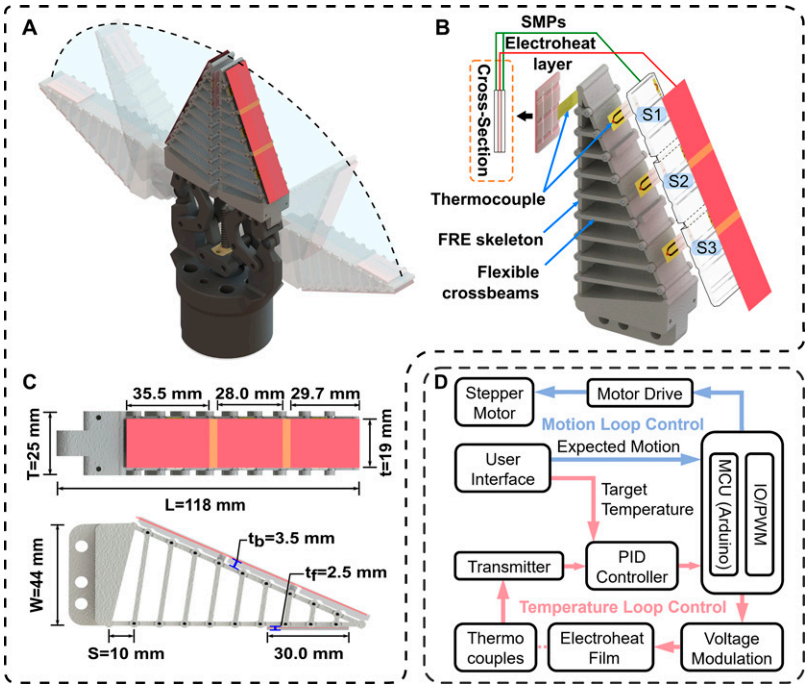

FIG. 3. Schematic diagram of the SMP-FRE gripper. **(A)** Illustration of the gripper's structure and workspace. **(B)** Exploded view of the SMP-FRE finger. **(C)** Detailed schematic of geometric parameters. **(D)** Layout of the electronic system configuration. FRE, Fin Ray Effect.

can serve as a plane of discontinuity, leading to stress concentrations and micro-crack propagation.[30] To address this, we opt for direct curing of E44 SMP onto the TPU substrate, allowing for uniform stress distribution and forming a stronger molecular bond between the SMP and TPU, which brings about improved structural integrity and durability.

The detailed fabrication process is shown in Figure 4. First, the flexible TPU skeleton and crossbeams are 3D printed using

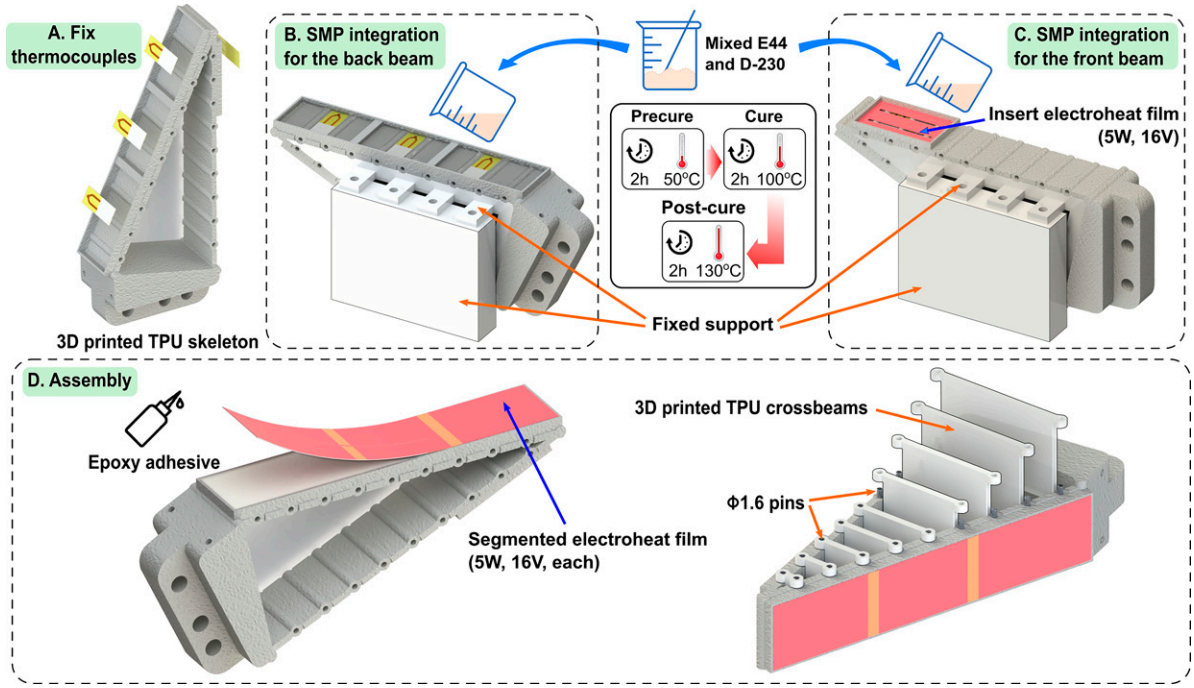

FIG. 4. Fabrication procedure of the SMP-FRE finger. **(A)** Print the TPU skeleton with SLS and paste the thermocouples. **(B)** Mix the epoxy monomer and curing agent D-230, pour the mixture into the back beam and pre-cure in the oven at 50°C for 2 h, cure at 100°C for 2 h and post-cure at 130°C for 2 h. **(C)** Integrate SMP with the front beam in the same way, meanwhile insert the electroheat film inside the material. **(D)** Assemble the fin ray finger with segmented electroheat film and TPU crossbeams. SLS, selective laser sintering; TPU, thermoplastic urethane.

a Multi Jet Fusion machine (HP) with TPU01 material. Thermocouples are affixed to the TPU skeleton before pouring the SMP to avoid temperature estimation errors due to thermal transmission delays. For the front beam, where surface smoothness is critical for adhesion-based grasping, the electroheat layer is preplaced on the skeleton surface. The SMP material is then cured on both the front and back beams following the mentioned curing conditions, with customized supports to prevent thermal deformation and ensure proper horizontal alignment. Finally, an epoxy adhesive secures the electroheat layer to the back beam of the FRE finger, and the assembly is completed by attaching the TPU crossbeams to the FRE skeleton.

Experiments and Results

The SMP-FRE robotic system, which integrates a 6-DOF robotic arm (UR5) with the proposed gripper, was designed to evaluate its enhanced versatility in grasping and manipulation. Specifically, the experiments assess improvements in load capacity, compliance across different force ranges, and the diversity of grasping modes available. Additionally, human-inspired strategies are explored for manipulating complex objects and grasping in confined environments.

Shape fixation and recovery assessment

The SMP-FRE gripper can reconfigure itself through intentional environmental interactions. The ability to maintain a modified shape after interaction and thermally recover is essential for stable operation and re-usability. This section quantitatively evaluates the finger's shape fixation and recovery abilities under various interaction conditions. As shown in Figure 5A, a single SMP-FRE finger is driven to interact with a plane. In particular, we investigate how contact angle and depth affect the ratio by measuring the displacement of the beam joints compared to the initial state.

The shape fixation experiment begins by heating the finger to above T_g, with the initial positions recorded. Upon the fingertip's contact with the plane, a downward load is applied until a predefined contact depth is reached. The joint positions in the contact state are recorded once the temperature reaches room temperature. The finger is then lifted from the surface, with the new configuration measured. By contrast, the shape recovery process starts from this locked state. The finger autonomously returns to its original configuration when reheated. Joint positions are continuously tracked throughout the recovery phase. Here, we define two metrics, the shape fixation ratio and the shape recovery ratio, to quantify shape retention and recovery capabilities, namely:

$$\begin{aligned} \mathrm{SFR} &= \frac{1}{N}\sum_{i=1}^{N}\frac{\left|\left|\mathbf{p}_i^{\mathrm{loc}}-\mathbf{p}_i^{\mathrm{ini}}\right|\right|}{\left|\left|\mathbf{p}_i^{\mathrm{con}}-\mathbf{p}_i^{\mathrm{ini}}\right|\right|} \\ \mathrm{SRR} &= \frac{1}{N}\sum_{i=1}^{N}\frac{\left|\left|\mathbf{p}_i^{\mathrm{rec}}-\mathbf{p}_i^{\mathrm{loc}}\right|\right|}{\left|\left|\mathbf{p}_i^{\mathrm{loc}}-\mathbf{p}_i^{\mathrm{ini}}\right|\right|} \end{aligned} \tag{1}$$

where $||\cdot||$ represents the Euclidean distance, N is the number of joints, and $\mathbf{p}_i^{\mathrm{ini}}$, $\mathbf{p}_i^{\mathrm{con}}$, $\mathbf{p}_i^{\mathrm{loc}}$, and $\mathbf{p}_i^{\mathrm{rec}}$ denote the initial joint position, joint position during contact, locked joint position, and joint position during recovery, respectively.

Results of the shape fixation experiment are shown in Figure 5B, covering three contact angles (0°, 30°, and 60°) and four loading depths (3, 6, 9, and 12 mm). The results indicate that stiffness modulation of the dorsal SMP well maintains the FRE finger's configuration across diverse interaction scenarios. Throughout all tests, the shape fixation ratio remained above 70%, even under large deformations, and exceeded 85% for contact depths below 6 mm. As contact angles and loading depths increase, the ratio decreases due to significant passive torque-induced compression within the crossbeams, which cannot be fully locked, leading to a discrepancy between the locked and interaction states. These results demonstrate the hand's capability to achieve reconfigurable interactions with the environment, enhancing its reliability in confined environments for successful grasping.

A shape recovery experiment following 30° contact angle and a 12 mm loading depth is further demonstrated, with the recovery temperature set to 80°C and a shape recovery ratio of 95% defined as the operational threshold. Owing to uniform heating during this stage, only the heating curve of the fingertip dorsal SMP is presented as a representative example. In Figure 5C, the SMP reaches the T_g at 79.45 s, and the whole finger recovers its shape in 318.95 s, with the recovered configuration closely matching the initial state. This result demonstrates SMP-FRE's excellent structure memory and recovery capabilities under controlled heating conditions, ensuring high operational efficiency and reliability over multiple usage cycles.

Enhanced shape adaptability and load handling capabilities

The FRE gripper, known for its inherent compliance, typically exhibits limitations regarding its load capacity and stability. The incorporation of SMP material can significantly expand its structural stiffness range, which allows the gripper to augment its load capacity and stability without sacrificing adaptivity, essential for manipulating objects with varying weights and shapes.

The shape adaptability and load capacity of the SMP-FRE gripper were evaluated through grasping tests in both low and high-stiffness modes. Figure 6A shows the gripper conforming to various objects, highlighting its gentle handling capabilities and good shape adaptability. Figure 6B shows its ability to handle items that require sufficient tip stiffness. In Figure 3C, the gripper successfully lifted 1000 and 500 g weights in high stiffness, while it can merely lift 100 g weight, with the 200 g weight slipping in low stiffness. Figure 6D and Supplementary Movie S2 illustrate the gripper's crushing force in high stiffness, greatly deforming a soda can, in contrast to the low stiffness state, which left the can undamaged. The experiment highlights the great stiffness variance of the SMP-FRE finger and its capability of handling diverse objects beyond what ordinary fin rays can achieve.

Interaction-driven reconfiguration for enhanced versatility

Conventional FRE grippers rely on passive deformation to envelop various objects but struggle with flat, thin, or tiny objects on planar surfaces and large convex objects due to the lack of specialized grasping mechanisms. Additionally, engaging with larger convex objects can be challenging due

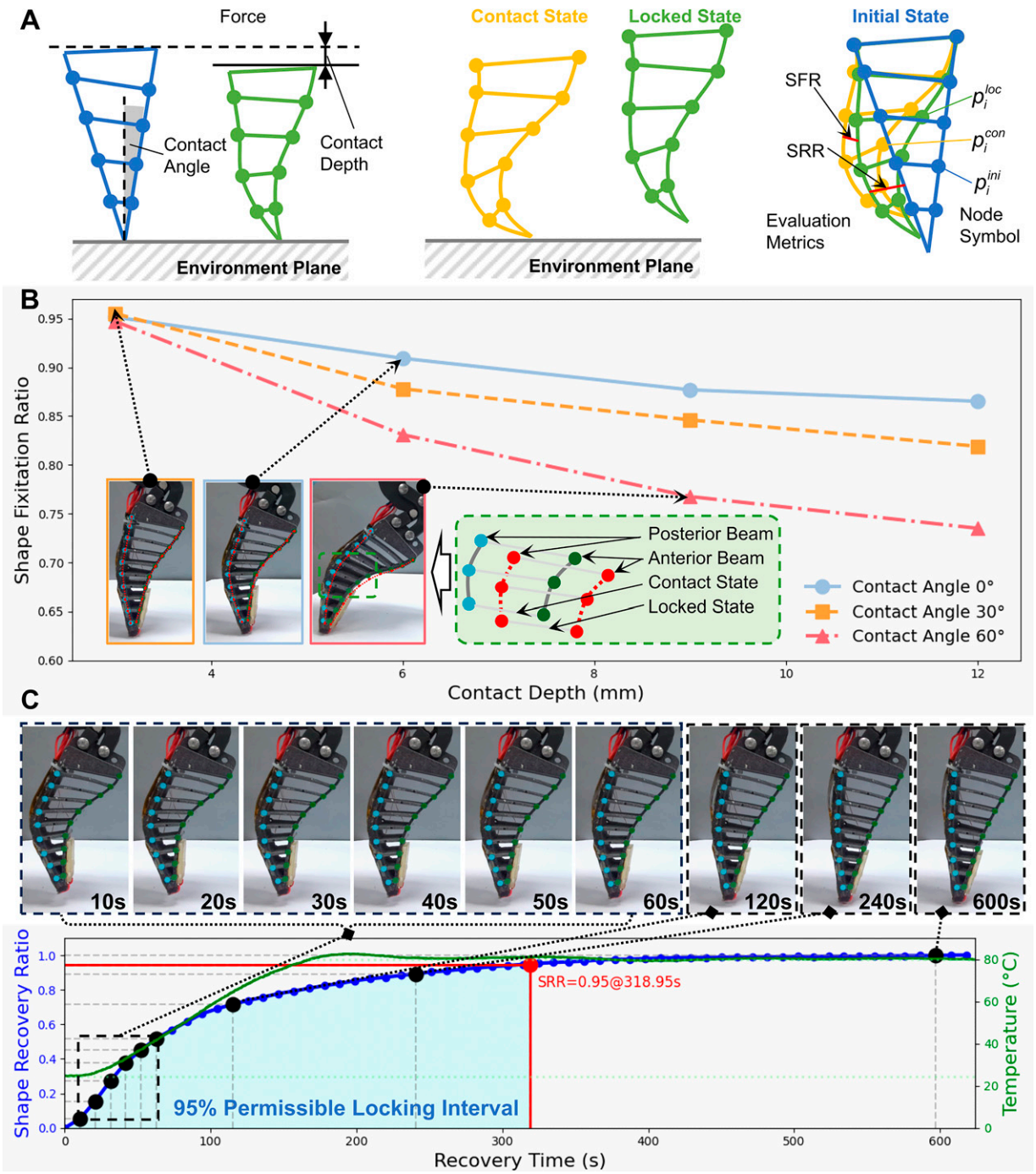

FIG. 5. Shape fixation and recovery capability experiments. **(A)** Schematic of the experimental principle, including quantitative loading conditions, interaction process, and description of evaluation metrics. **(B)** Results of the shape locking capability experiment, demonstrating SFR measurements of the SMP-FRE finger at various interaction angles and depths. **(C)** Results of the shape recovery capability experiment, demonstrate SRR measurements of the SMP-FRE finger as it autonomously returns to its initial state after heating from the locked state, along with the corresponding temperatures. SFR, shape fixation ratio; SRR, shape recovery ratio.

to an insufficient grasping angle. The integration of SMP significantly enhances performance. For large-radius, thin, or tiny objects, the back beam remains stiff to apply sufficient preload, while the front beam's adhesion secures the grip. For concave surfaces, heating the gripper above T_g allows the front beam to conform to the shape, and once cooled, the front SMP provides stable adhesion. This flexibility enables conformal adhesive contact with diverse surface shapes, improving grasp stability and robustness. As shown in Figure 7A and Supplementary Movie S1, the gripper successfully grasped an acrylic semi-sphere, a basketball, a 14-inch plate, an A4 sheet of paper, a thin ID card, and M5 nuts.

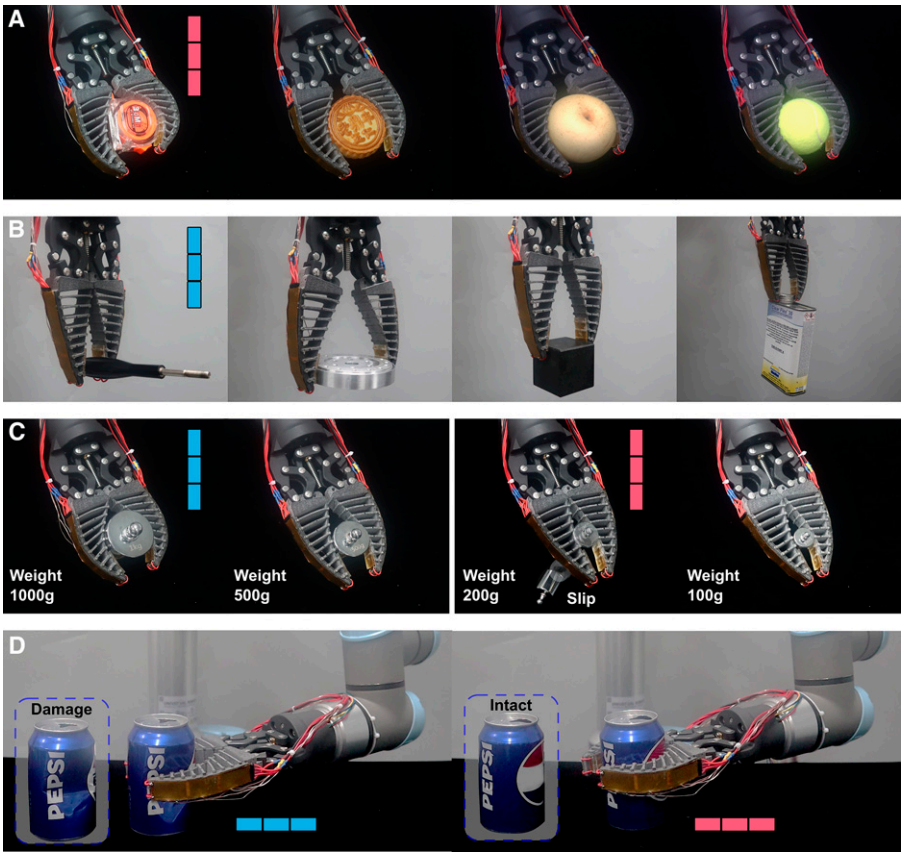

FIG. 6. Demonstration of the SMP-FRE gripper's adaptability and load capacity, with color indicating SMP stiffness distribution (*red*: soft state; *blue*: stiff state). **(A)** Low stiffness mode: The SMP-FRE gripper conforms to objects with various shapes including a tape measure (83.5 g), a mooncake (82.8 g), a pear (280.7 g) and a tennis ball (58.6 g), showcasing its adaptability for gentle handling. **(B)** High stiffness mode: The SMP-FRE gripper exhibits sufficient load-bearing capacity and gripping force to securely grasp objects including a screwdriver (25.5 g), a flange (304.3 g), a metal block (423.8 g) and a metal can (548.8 g). **(C)** Load-bearing capacity comparison: at high stiffness, the gripper can successfully lift 500g and 1000 g weights, whereas, at low stiffness, it can only securely grasp 100 g weights, with 200 g weights slipping. **(D)** Impact assessment on a soda can: when applying maximum force, high stiffness results in significant deformation, while low stiffness preserves the can's integrity.

The dorsal SMPs significantly enhance the grasping and manipulation capabilities of the gripper by enabling interaction-driven reconfiguration. We simplify this interaction by considering a two-phalange gripper, one soft and one rigid, as illustrated in Figure 7B. Soft robots, due to their joint compliance, effectively interact with their environment and achieve grasping under environmental constraints. However, their grasping force is entirely determined by joint stiffness, often leading to failure due to insufficient tip stiffness. Conversely, conventional rigid grippers struggle with environmental interaction and require precise kinematic planning for successful grasping, risking damage to the hand. We experimentally validated the benefits of variable stiffness for the FRE hand. As shown in Figure 7C and Supplementary Movie S3, we evaluated improvements in shear grasping force using a steel ball (1180 g). Pure stiff and flexible states failed due to insufficient contact area and grasping force. In contrast, our gripper, leveraging a soft-interaction-stiff-grasping strategy, significantly increased contact area while maintaining load capacity. Additionally, variable stiffness aids in operating tools in real-world scenarios. Inspired by human grasping and tool-using, we demonstrate the

FIG. 7. Demonstration of the enhanced capabilities and strategies for object grasping and manipulation, with color indicating SMP stiffness distribution (red: soft state; blue: stiff state). **(A)** Grasping of an acrylic semi-sphere with a diameter of 300 mm (296 g), a basketball with a diameter of 246 mm (600 g), a 14-inch plate (540 g), a sheet of A4 paper (4.5 g), an ID card (6.4 g) and M5 nuts (one weighing 6.6 g) with SMP adhesion. **(B)** Comparison of interaction mechanisms between a simplified soft and rigid gripper during object grasping from constrained surfaces. **(C)** Enhanced grasping and manipulation through sophisticated robot-object interactions. The gripper can interact with objects to achieve the grasping of a steel ball (1180 g) and the manipulation of a hand drill. **(D)** Robotic environmental interaction for Versatile Grasping Reconfiguration. Through interacting with the desktop or box frame, the gripper can alter its configuration to perform human-like actions including precise pinching, hooking, and corner grasping.

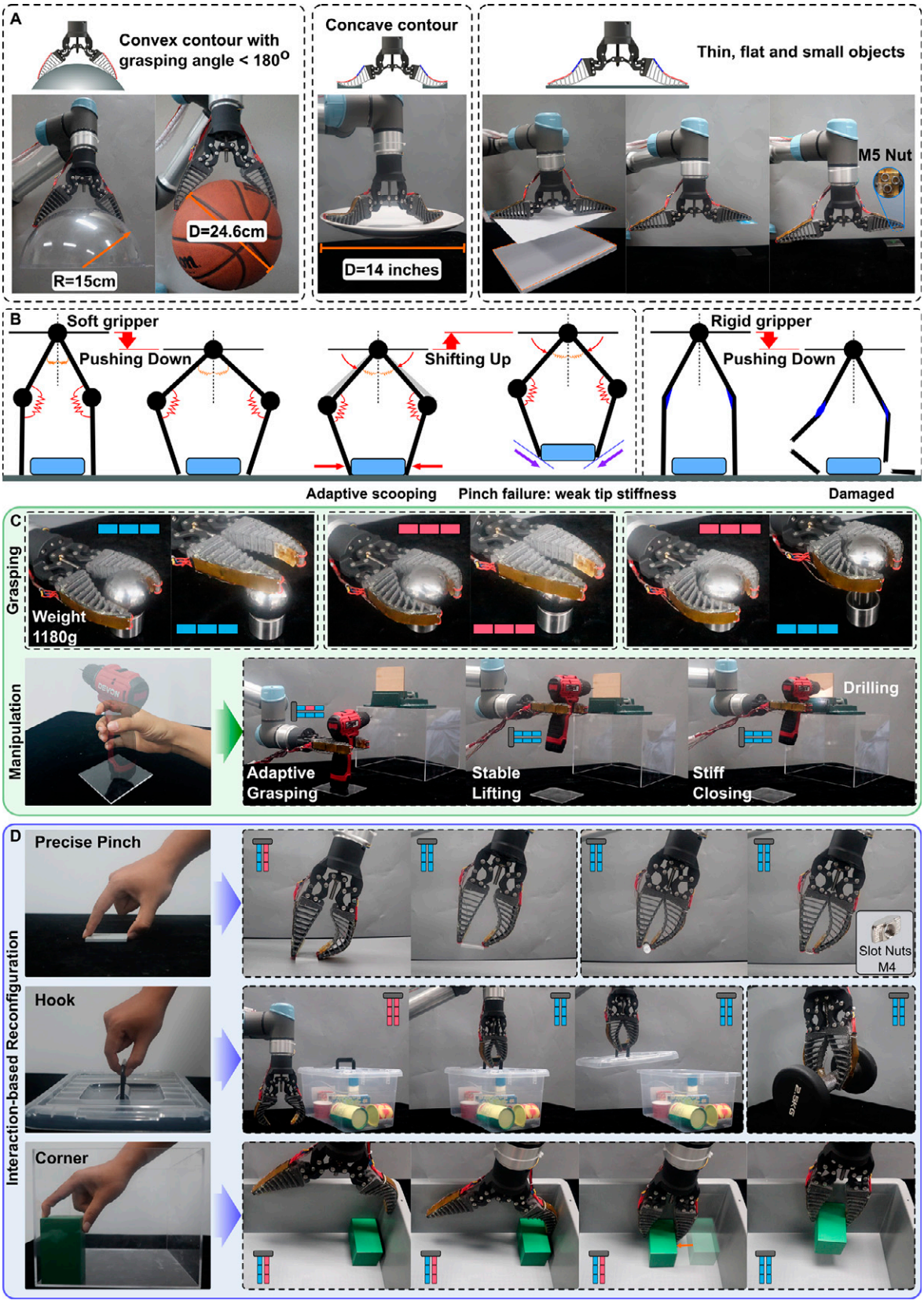

gripper's functionality using a hand drill. To stabilize the grasp without triggering the switch, we selectively heated the middle section of the back beam to reduce interaction force, then cooled it to enhance grasp stability. The gripper was further closed upon approaching the target to activate the switch while maintaining stability. This human-like strategy enabled successful drilling into a 3 mm wooden board.

Furthermore, we evaluated the grasping performance of the proposed gripper using human-inspired interaction strategies in various constrained scenarios. As previously noted, grasping thin objects from flat surfaces often requires specialized designs and careful grasp planning.[4] The proposed hand utilizes reconfigurable and lockable soft interactions with the environment, allowing for flexible change in its workspace and achieving precise pinching actions through scooping. Figure 7D and Supplementary Movie S4 illustrate the gripper successfully picking a thin plate, a pen, and a slot nut from a table. Moreover, when both fingers are in a flexible state, the interaction with the environment can dynamically alter the tip orientation, allowing for a human-like hook configuration that stably manages objects with handles. This configuration has been further validated for shoulder dumbbells weighing 2.5 kg (50 times its weight). Besides, inspired by human grasping objects trapped in corners, the tip of the FRE finger can engage with walls, allowing it to slide into gaps between objects and the wall, as seen in Supplementary Movie S5. During this adaptive closing process, the hand effectively translates the object and achieves a stable grasp upon cooling into a rigid state. This approach highlights the hand's versatility in real-world scenarios, ensuring secure handling in complex environments.

Conclusion

To conclude, this study introduces a novel paradigm that utilizes the thermo-responsive stiffness and reversible adhesion of SMP materials to augment the grasping modality in FRE gripper design. The integration of SMPs not only expands the range of stiffness variations by tens of times while preserving its adaptability but also facilitates the capability of grasping large-radius, thin, or tiny objects through adhesion-based mechanisms. Besides, the gripper excels at handling a broad spectrum of objects while also securing excellent grasping performance in constrained environments. Inspired by human grasping and manipulation strategies, the gripper actively modifies its configuration to handle complex tasks with minimal complexity. This work proposes a novel solution for multifunctional grasping in soft robotics, addressing the pressing need for compliance, precision, and load-carrying in real-world applications. Future efforts will explore the integration of active cooling mechanisms to improve cooling efficiency, as well as the development of autonomous reconfiguration strategies based on theoretical modeling, pushing the boundaries of reconfigurable robotic systems.

Author Disclosure Statement

No competing financial interests exist.

Authors Contributions

H.G., H.W., and Y. W. conceived the idea. H.W. and H.G. developed the methods and fabrications for the SMP-enhanced FRE finger. Y.W. designed the gripper. H.G. and H.W. developed the control system of the gripper. H.W., Y.X., and T.W.W. conducted the characterization of the prepared SMP samples. Y.W., H.G., and H.W., performed the shape fixation and recovery assessment. H.G., H.W., and Y.W. conducted the grasping evaluation of the proposed gripper. H.G., H.W., and Y.W. wrote the manuscript with input from all authors. H.D. and Y.W. provided the fundings for this work. The study was supervised by H.D. and T.L.

Funding Information

The authors gratefully acknowledge the financial support from the National Key Research and Development Program of China (Grant no. 2023YFB4704700), National Natural Science Foundation of China through the Youth Program (Grant no. 509109-N72401), the China Postdoctoral Science Foundation (Grant no. 2024M762814), Zhejiang Provincial Natural Science Foundation (Grant no. LD24E050006), and Science and Technology Bureau of Ningbo City (Grant no. 509109-W02502).

Supplementary Material

Supplementary Movie S1
Supplementary Movie S2
Supplementary Movie S3
Supplementary Movie S4
Supplementary Movie S5

References

1. Cui Y, Liu X-J, Dong X, et al. Enhancing the universality of a pneumatic gripper via continuously adjustable initial grasp postures. IEEE Trans Robot 2021;37(5):1604–1618.
2. Zhang Y, Zhang N, Hingorani H, et al. Fast-Response, Stiffness-Tunable soft actuator by hybrid multimaterial 3D printing. Adv Funct Mater 2019;29:1806698.
3. Yang Y, Chen Y, Li Y, et al. Bioinspired robotic fingers based on pneumatic actuator and 3D printing of smart material. Soft Robot 2017;4(2):147–162.
4. Babin V, Gosselin C. Picking, grasping, or scooping small objects lying on flat surfaces: A design approach. Int J Rob Res 2018;37(12):1484–1499.
5. Manti M, Cacucciolo V, Cianchetti M. Stiffening in soft robotics: A review of the state of the art. IEEE Robot Automat Mag 2016;23(3):93–106.
6. Halsey TC. Electrorheological fluids. Science 1992;258(5083): 761–766.
7. Crowley GB, Zeng X, Su H-J. A 3D printed soft robotic gripper with a variable stiffness enabled by a novel positive pressure layer jamming technology. IEEE Robot Autom Lett 2022;7(2):5477–5482.
8. Brown E, Rodenberg N, Amend J, et al. Universal robotic gripper based on the jamming of granular material. Proc Natl Acad Sci USA 2010;107(44):18809–18814.
9. Zhao R, Yao Y, Luo Y. Development of a variable stiffness over tube based on low-melting-point-alloy for endoscopic surgery. Journal of Medical Devices 2016;10(2):21002.

10. Wang W, Yu CY, Abrego Serrano PA, et al. Shape memory alloy-based soft finger with changeable bending length using targeted variable stiffness. Soft Robot 2020;7(3): 283–291.
11. Firouzeh A, Salerno M, Paik J. Stiffness control with shape memory polymer in underactuated robotic origamis. IEEE Trans Robot 2017;33(4):765–777.
12. Firouzeh A, Paik J. Grasp mode and compliance control of an underactuated origami gripper using adjustable stiffness joints. IEEE/ASME Trans Mechatron 2017;22(5):2165–2173.
13. Linghu C, Zhang S, Wang C, et al. Universal SMP gripper with massive and selective capabilities for multiscaled, arbitrarily shaped objects. Sci Adv 2020;6(7):eaay5120.
14. Peng J, Xie S, Liu T, et al. High-performance epoxy vitrimer with superior self-healing, shape-memory, flame retardancy, and antibacterial properties based on multifunctional curing agent. Composites Part B: Engineering 2022;242: 110109.
15. Tonazzini A, Sadeghi A, Mazzolai B. Electrorheological valves for flexible fluidic actuators. Soft Robot 2016;3(1): 34–41.
16. Jing H, Hua L, Long F, et al. Variable stiffness and fast-response soft structures based on electrorheological fluids. J Mater Chem C 2023;11(35):11842–11850.
17. Atakuru T, Züngör G, Samur E. Layer Jamming of Magnetorheological Elastomers for Variable Stiffness in Soft Robots. Exp Mech 2024;64(3):393–404.
18. Shintake J, Schubert B, Rosset S, et al. Variable stiffness actuator for soft robotics using dielectric elastomer and low-melting-point alloy, in *2015 IEEE/RSJ International Conference on Intelligent Robots and Systems (IROS)*, pp. 1097–1102, 2015.
19. Xia Y, He Y, Zhang F-h, et al. A review of shape memory polymers and composites: Mechanisms, materials, and applications. Adv Mater 2021;33(6):e2000713.
20. Park JK, Eisenhaure JD, Kim S. Reversible underwater dry adhesion of a shape memory polymer. Adv Mater Interfaces 2019;6(1801542).
21. Al Abeach LA, Nefti-Meziani S, Davis S. Design of a variable stiffness soft dexterous gripper. Soft Robot 2017;4(3): 274–284.
22. Konda R, Bombara D, Swanbeck S, et al. Anthropomorphic twisted string-actuated soft robotic gripper with tendon-based stiffening. IEEE Trans Robot 2023;39(2):1178–1195.
23. Yao J, Fang Y, Yang X, et al. Design optimization of soft robotic fingers biologically inspired by the fin ray effect with intrinsic force sensing. Mech Mach Theory 2024;191:105472.
24. Wang H, Gao B, Hu A, et al. A variable stiffness gripper with reconfigurable finger joint for versatile manipulations. Soft Robot 2023;10(5):1041–1054.
25. Chen R, Song R, Zhang Z, et al. Bio-Inspired Shape-Adaptive soft robotic grippers augmented with electroadhesion functionality. Soft Robot 2019;6(6):701–712.
26. Liu X, Han X, Hong W, et al. Proprioceptive learning with soft polyhedral networks. Int J Rob Res 2023;0(0).
27. Wang X, Wang B, Pinskier J, et al. Fin-bayes: A multi-objective bayesian optimization framework for soft robotic fingers. Soft Robot 2024;0(0).
28. Kashef Tabrizian S, Terryn S, Brauchle D, et al. Variable stiffness, sensing, and healing in festo's finray gripper: An industry-driven design. IEEE Robotics Automation Magazine 2024:2–13.
29. Shan X, Birglen L. Modeling and analysis of soft robotic fingers using the fin ray effect. Int J Rob Res 2020;39(14): 1686–1705.
30. Liu H-L, Lin C-L, Sun M-T, et al. 3D Micro-Crack propagation simulation at enamel/adhesive interface using FE submodeling and element death techniques. Ann Biomed Eng 2010;38(6):2004–2012.

Address correspondence to:
Huixu Dong
Grasp Lab of Mechanical Engineering Department
Kaiwu Yuan 3
Zijingang Campus
Zhejiang University
Hangzhou
310058
China

E-mail: huixudong@zju.edu.cn